Preprints of the 2012 20th Mediterranean Conference on Control & Automation (MED), Barcelona, Spain, July 3-6, 2012

Feed-forward friction observer (FFFO) for high-dynamic motion control

Michael Ruderman and Torsten Bertram

Abstract— **The dynamic friction in motion systems is mostly not directly measurable and has to be observed for an efficient compensation. A novel feed-forward friction observer (FFFO) is proposed based on the two-state dynamic friction model with elasto-plasticity abbreviated by 2SEP friction model. Being involved in the underlying closed control loop the FFFO uses the control error to adjust the friction dynamics which is computed in feed-forwarding based on the reference velocity. The friction compensation is evaluated on the actuated motion system with multiple coupled frictional surfaces. The proposed FFFO approach proves to be superior in comparison to the common friction observer which uses the output velocity value.**

I. INTRODUCTION

Considering the problem of friction compensation in motion control systems different model-based approaches can be pursued. Historically, the methods of friction compensation were developed collateral with the control-oriented friction models. A former survey on friction modeling and compensation can be found in [1]. The most elaborated dynamic friction models, among Dahl, LuGre, Leuven, and Generalized Maxwell-Slip (GMS), can be applied in a feed-forward manner to overcome the nonlinear friction, particularly in the presliding regime [2]. However, since one tackles the dynamic friction problem in a large varying velocity range a pure feed-forwarding exhibits certain lacks due to its limited generality. Here rather the adaptive or observer-based compensation schemes are in demand. Due to a compact parametrization and continuous representation of the single-state friction dynamics the LuGre friction model [3], [4] became the most favored one for such purposes. Also the recently developed two-state dynamic friction model with elasto-plasticity (2SEP), first introduced in [5], can be applied in various control schemes.

To the best of our knowledge, a proper adaptive model-based friction compensation in terms of an online tuning of the frictional parameters is rare. Let us recall that an adjustment of the dynamic friction parameters and not of a static friction characteristic curve only is meant. Here the main challenge consists in the proof of stability required to guarantee the boundedness of all signals and states during the continuous parameter adaptation. An auto-tuning feed-forward friction compensation using the gradient-based algorithm and LuGre friction model has been proposed and experimentally evaluated in [6]. However, the special adaptation gains and predefined reference signals have been presupposed to restrict the parameters within a domain.

M. Ruderman and T. Bertram are with the Institute of Control Theory and Systems Engineering, Technische Universität Dortmund, 44221-Dortmund, Germany, mykhaylo.ruderman@tu-dortmund.de

More attractive, at least from a stability point of view, is to apply a friction observer as proposed e.g. in [7] for the LuGre friction model. Different observer-based friction compensators can be thinkable while the design of an appropriate observation function is the main task to be solved. Several friction observers use the closed-loop control error to adjust the dynamic friction state. Alternatively, a Luenberger-type friction observer can be applied as proposed in [8]. This scheme provides an accurate friction estimate simultaneously with the overall system dynamics. However, note that the prediction error of system output is used for observing an internal friction state. Hence the computed compensation signal injected to the control value exhibits an abiding lag regarding the actual friction of the plant. This restricts the response time of the friction estimate and bandwidth of the applicable reference values. Another observer-based and adaptive compensation schemes have been proposed e.g. in [9], [10], [11] using the Maxwell-slip oriented friction modeling. In [9], particularly the compensation of an initial friction behavior has been addressed in order to solve the fast and precise positioning tasks. The motion control presented in [10] combines the friction model feed-forwarding with an inverse model-based disturbance observer. Both parts of the proposed compensator imply the GMS friction model. An adaptive approach presented in [11] uses the DNLRX friction model which can be considered as a time-series extension of an underlying Maxwell-slip-based modeling approach. The method involves a recursive least-squares algorithm to adapt the linear DNLRX parameters.

The novel feed-forward friction observer (FFFO) introduced in this work applies the 2SEP friction model [5], [12] and is basically inspired by the observation strategy presented in [13]. On the other hand, the permanent control lag detected experimentally gives us the idea of computing the dynamic friction based on the reference and not control velocity value. But while doing so the friction estimate is driven by the closed-loop control error similarly as in [13]. We suppose that uncertain frictional adhesions and time delays, both present in a real motion system, restrict the efficiency of a friction observation when using the measured output value. Thus, the proposed "combined" strategy aims to joint the rapidness of the friction computation in feed-forwarding with an observation of the real friction state. In the following, the friction observation using 2SEP friction model is addressed. The control structure including the proof of stability is provided. The experimental evaluation of the FFFO-based control in comparison to the reference linear feedback control and observer-based control which uses the output velocity is described in details.

978-1-4673-2529-5/12/$31.00 ©2012 IEEE

II. FRICTION OBSERVATION WITH 2SEP MODEL

The two-state dynamic friction model with elasto-plasticity abbreviated by 2SEP friction model describes the overall friction force (torque) as a superposition

$$F(t) = A\, z_1(t) + B\,\big|w(t)\big|\, z_2(t) \tag{1}$$

of one pre-sliding hysteresis state and one transient dynamic state weighted by A and B correspondingly. The pre-sliding friction dynamics [14] is driven by

$$\dot{z}_1(t) = |\Omega|\, w(t)\, K \exp\Big(-K\big|x_r(t)\big|\Big) \tag{2}$$

with

$$x_r(t) = \int_{t_r}^{t} w(t)\,\mathrm{d}t\,, \tag{3}$$

where

$$\Omega = \operatorname{sgn}(w)\, F_c - F(t_r) \quad \text{and} \quad x_r(t_r) = 0 \tag{4}$$

whenever the sign of the relative velocity $w(t)$ changes at t_r. F_c is the constant Coulomb friction and K is the initial stiffness of interacting asperities upon the frictional surfaces. When assuming that an elasto-plastic asperity deflection saturates at the Coulomb friction level the weighting factor A can be set to one (see [14] for details) thus reducing the number of free parameters.

The transient friction response is given by

$$\dot{z}_2(t) = \frac{S(w) - F(t)}{\big|S(w)\big|}\,, \tag{5}$$

where the velocity-dependent steady-state friction $S(w) = s(w) + \sigma w$ includes the Stribeck characteristic curve $s(w)$ and viscous linear friction term captured by σ. The state equation (5) serves as an attractor of the overall friction dynamics towards the steady-state characteristic curve. For more details to 2SEP friction model we refer to [12], [14].

Due to the linear state combination the overall friction state can be observed by

$$\dot{\hat{F}}(t) = \dot{\hat{z}}_1(t) + B\big|w(t)\big|\dot{\hat{z}}_2(t) + \lambda\big(e(t)\big) \tag{6}$$

where the control error $e = w_r - w$ serves as the argument of a positive definite observation function $\lambda(\cdot)$. Note that since $|w|$ in (1) is an external weighting factor and the $\dot{z}_2$ dynamics is a function of the static $S(w)$ map and dynamic $F(t)$ value only the chain rule of differentiation in not applied when obtaining the right-hand side second term in (6). The hat notation ($\hat{}$) denotes the estimated (modeled) friction values. Recall that the modeled friction can be computed using either the control $w(t)$ or reference $w_r(t)$ velocity value as will be shown further in Section III. Since the friction appears as a damping factor of the motion system a positive control error means an undercompensated friction disturbance. For this reason $\lambda(\cdot)$ term contributes with a positive sign in (6).

Using (1), (5), and (6) one obtains

$$\dot{\hat{F}}(t) + \frac{B\big|w(t)\big|}{\big|S(w)\big|}\,\hat{F}(t) = \dot{\hat{z}}_1(t) + B\,w(t) + \lambda\big(e(t)\big)\,. \tag{7}$$

It is easy to recognize that the left-hand side of (7) constitutes a first-order time-delay element with a velocity-dependent but always non-negative time factor $\big|S(w)\big|/B|w|$, the parameter $B > 0$ assumed. Hence, a stable eigenbehavior of the friction estimate is ensured independent of the selected observation function which contributes as an excitation on the right-hand side of (7). Recall that through the damping term the modeled dynamic friction captures the well-known frictional lag [15]. The frictional lag arises as a time delay between the non-constant relative velocity and friction force.

When the observation error is zero, i.e. $e = 0 \rightarrow \lambda = 0$, the overall friction dynamics is excited by $\dot{\hat{z}}_1$ and relative velocity only. Note that since an elasto-plastic transition reaches its saturated state ($\dot{\hat{z}}_1 = 0$) relatively fast, during an unidirectional motion, the excitation of $\dot{\hat{F}}$ dynamics occurs under nearly step-like conditions. Afterwards, it is the variable relative velocity and control error (when not zero) which drive the dynamic friction estimate. Recall that the first-order time-delay behavior of the dynamic friction serves as a low-pass filter. Thus, a high-frequent process or measurement noise, both reflected in the control error, can not distort substantially the estimated friction state.

III. MOTION CONTROL WITH FRICTION OBSERVER

A. Control structure

The motion control system with friction observer which is involved in the velocity feedback loop is shown in Fig. 1. Note that here the linear feedback controller $R(p)$ and

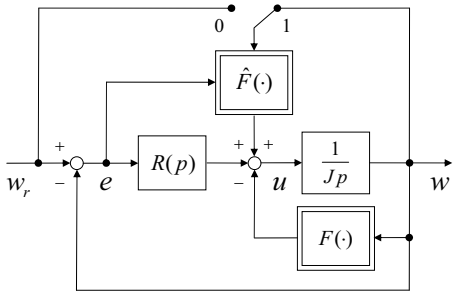

Fig. 1. Friction observer enclosed in the velocity control loop. The toggle [0, 1] switches between the feed-forward and feedback friction observer

forward integral part are denoted in the Laplace domain using the p variable. The linear control, either PI or PID one, has to be designed possibly robust for the considered operation range. The relative velocity w of the inertial mass J is mainly damped through the nonlinear friction F. The computed dynamic friction $\hat{F}$ which is auxiliary observed using the control error e (as described before in Section II) injects the control signal u. Thus the overall control law obtains two degrees-of-freedom. Note that in the shown control scheme the friction value can be computed using either the reference or measured velocity signal, depending on the toggle switch set to "0" or "1" correspondingly.

In [13], an observer-based friction compensation has been shown while computing the dynamic friction based on the

measured relative velocity and using the LuGre friction model. The authors showed that the map between the control error and $F-\hat{F}$, which is the error of friction estimate, is dissipative with respect to the dynamic friction state. Further, it has been proved that the linear control $R(p)$ with an integral action (e.g. PI or PID one) can guarantee the asymptotic stability of the control system with friction observer. This is under conditions that $1/R(p)$ is positive real for all frequencies and has no poles on the imaginary axis. Also it has been shown that if $w_r \neq 0$ then $(F-\hat{F}) \to 0$.

B. Proof of stability and boundedness

To prove the stability of the closed control loop and the boundedness of internal signals related to the feed-forward compensation, which is a function of both reference value and control error, consider the motion system

$$J\dot{w}(t) = u(t) - F\big(w(t)\big) + \hat{F}\big(w_r(t)\big)\,. \tag{8}$$

After substituting the linear PI control

$$u(t) = K_p\big(w_r(t) - w(t)\big) + K_i \int \big(w_r(t) - w(t)\big)\,dt \tag{9}$$

into (8) and reforming the resulted equation and derivating with respect to time one obtains

$$J\ddot{w} + K_p\dot{w} + K_i w = K_p\dot{w}_r + K_i w_r + \dot{\hat{F}}(w_r) - \dot{F}(w)\,. \tag{10}$$

Note that in (10) and later the time argument is omitted for the sake of simplicity. Considering a simple case observation function $\lambda(e) = Le$ and using the friction time derivative from (6) one obtains the motion dynamics as

$$J\ddot{w} + K_p\dot{w} + (K_i + L)w + \dot{F}(w) = x\,, \tag{11}$$

with the right-hand side excitation function

$$x = K_p\dot{w}_r + (K_i + L)w_r + \dot{\hat{z}}_1 + B|w_r|\dot{\hat{z}}_2\,. \tag{12}$$

Since all the summands in (12) are computed using the reference value only and furthermore bounded, the overall boundedness of the system excitation is ensured.

To prove the asymptotic stability of the motion system (11) the dynamical friction contribution has to be analyzed, assuming all the residual constants $[J, K_p, K_i, L] > 0$. Taken into account the state dynamics (2) and (5) and the $|w|$ contribution in (1) the friction dynamics is approximated by

$$\dot{F}(w) = C_1(F)\,w + C_2(F,w)\,w\,. \tag{13}$$

It can be shown that due to the exponential term in (2) and a variable $|\Omega|$ value the first coefficient of the linear approximation (13) fulfills $0 \le C_1 \le 2F_cK$. With respect to zero-velocity transitions the second coefficient can vary as $-2B \le C_2 \le 2B$. When substituting (13) into (11) it can be seen that the control parameters must satisfy

$$K_i + L \ge 2B\,, \tag{14}$$

in order to guaranty an asymptotic stability of the motion system over the total velocity and friction range.

IV. CONTROL DESIGN AND EVALUATION

A. Experimental motion setup

The experimental setup taken for the control evaluation is shown in Fig. 2 (a). The motion system with one rotary degree-of-freedom contains a standard BLDC motor with the rated power 400 W and idling speed 3100 rpm. The servo drive is equipped by a 15-bit resolver and is energized through a PWM electronic unit containing an onboard current controller of 11 kHz rate. All the input and output signals provided to the external real-time control unit in use are sampled with 2 kHz rate.

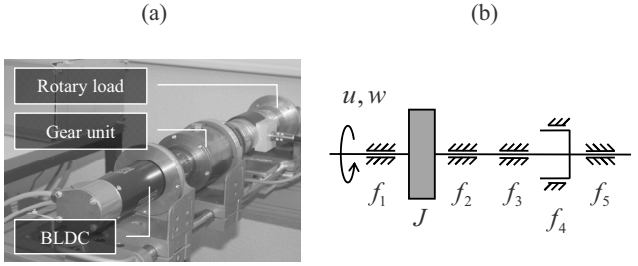

Fig. 2. Experimental motion setup with one rotary degree-of-freedom (a) and equivalent structure with multiple frictional surfaces (b)

The BLDC motor drives a high reducing gear unit (160:1) whose elasticities can be neglected insofar as it provides a high structural damping and a relative high stiffness in relation to the output load torques. Hence, the lumped system inertia J can be assumed as sketched in Fig. 2 (b). The motion setup offers multiple coupled frictional surfaces distinguished as f_1–f_5. Here f_4 represents the teeth interaction of the gear and the residuals are of the ball bearing type.

B. System identification

To identify the motion system with nonlinear friction the specially designed input sequence depicted in Fig. 3 (a) is applied. The input sequence constitutes a concatenation

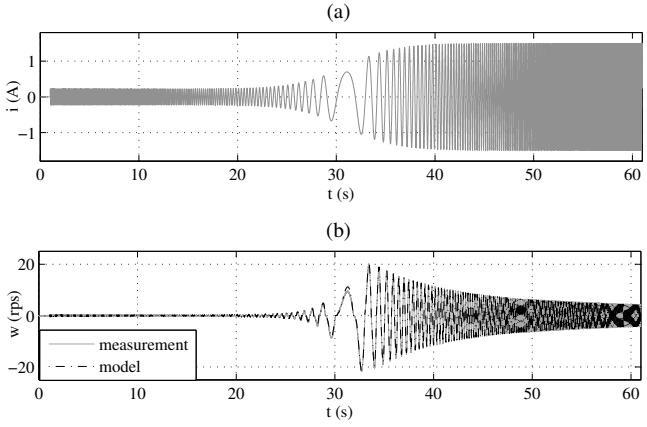

Fig. 3. Excitation current sequence (a), relative velocity response (b)

of one down-chirp and one up-chirp signal with the bandwidth between 0.01 Hz and 10 Hz, both enveloped by a biased sigmoid function. The applied excitation provokes

the frictional behavior in both, pre-sliding (within several degrees only) and sliding regime and that for relative low and high frequencies. The measured velocity response is shown together with the identified model in Fig. 3 (b).

The system dynamics described by

$$J\dot{w}(t) + F\big(w(t)\big) = u(t - T_d) \tag{15}$$

has been identified in a least-squares sense using the measured and computed relative velocity. The input torque u is assumed to be proportional to the controlled motor current i. Note that the identified time delay T_d, mandatory assumed due to the digital motor control, amounts for 3 ms that corresponds to six sampling times and can not be fully neglected. The identified parameters of 2SEP friction model

TABLE I
IDENTIFIED FRICTION PARAMETERS

Param.	σ	F_c	F_s	V_s	δ	K	B
Unit	Nm/rps	Nm	Nm	rps	-	$0.5/\pi$	1/rps
Value	0.003	0.025	0.067	0.733	-1.07	778	2.33

are listed in Table I (see [8] for residual parameter notation).

Analyzing the residual model errors depicted in Fig. 4 it can be seen that the error spread in negative direction is larger than that in positive one. The error distribution reveals the

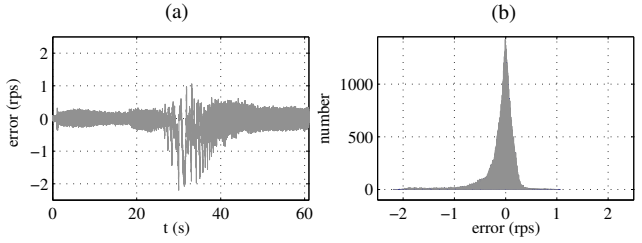

Fig. 4. Residual model errors as time series in (a) and histogram in (b)

system behavior as slightly unsymmetric depending on the velocity sign, – the issue which is not captured by the model. Apart from that the residual model errors are well distributed reciprocal to zero. Furthermore it can be recognized that the model errors at lower frequencies are larger than those at higher frequencies and that for low and high amplitudes. This can be explained by the model uncertainties owing to the frictional adhesion mechanisms that gains in importance at lower frequencies. Note that lower excitation frequencies lead correspondingly to the lower accelerations at which the dwell times [16] increase and the frictional conditions at the motion onset can vary to a larger extent.

C. Robust feedback control design

The linear velocity-feedback control is designed in a robust manner by analyzing the estimated frequency response function (FRF) of the motion system at higher excitation amplitudes. The corresponding FRF is obtained by applying the down-chirp excitation with a bandwidth 50–0.01 Hz. Afterwards, the first-order linear approximation of the plant is fitted using the experimental FRF data. The computed FRF of the identified linear approximation is shown versus the measurement in Fig. 5. Note that for identifying the FRF the amplitude response only has been used due to a large discrepance detected in the measured phase response. This one ca be attributed to the nonlinear friction lag whose impact on the phase response drops to a larger extent at higher frequencies (see [12] for details). The resulting transfer function of the

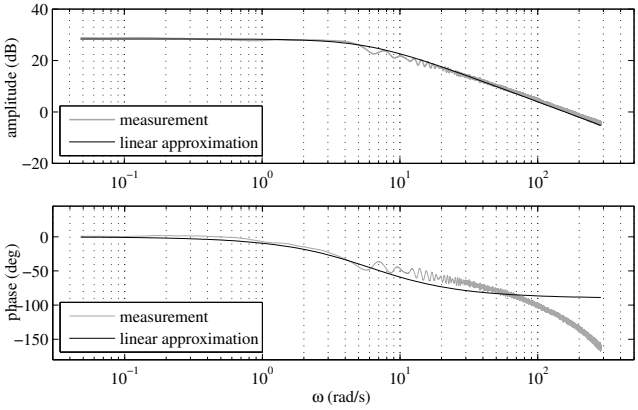

Fig. 5. Measured and linear approximated frequency response function

open control loop with the PI regulator is

$$R(p)H(p) = \frac{K_p(T_i\,p+1)}{T_i\,p}\,\frac{G_h}{T_h\,p+1}\,, \tag{16}$$

where the control gain K_p and integral time constant T_i constitute the regulator parameters to be tuned. The determined values $G_h = 26.17$ and $T_h = 0.166$ are the gain and time constant of the linear plant approximation. With respect to the time constant and actuator boundaries the integral time constant has been set to $T_i = 0.1$.

Robustness of the designed feedback control loop is illustrated using the root locus diagram depicted in Fig. 6. It is assumed that uncertainties related to the friction are predominant in comparison to those related to the inertia and time delay of the motion system (15). Thus, the robustness of the control loop is crucial with regard to the nonlinear damping which is conditioned by the friction. As shown in [12] the overall frictional damping D depends rigorous on the ongoing excitation amplitude so that the transfer function can be rewritten as

$$H(p,|U|) = \frac{1/D\big(|U|\big)}{pJ/D\big(|U|\big)+1}\,. \tag{17}$$

Since the frictional damping contributes to the numerator of (17) the total gain $\mathrm{G} = K_p D^{-1}$ of the open control loop can be seen as a measure of uncertainties. Note that the impact of D on the eigenbehavior is so that the pole indicated by T_h in Fig. 6 will be solely shifted along the real axis. The pole goes to the left when the damping increases and to the right when the damping decreases. Regarding several sample points indicated in Fig. 6 it can be seen that the gain variation

between 0.17 and 6.5 (that is about 40 times) results in a still effectual control behavior without transient overshoot. Note that the indicated zero at T_i constitutes the right-hand

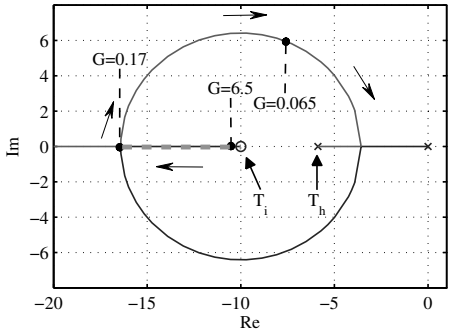

Fig. 6. Root locus of the linear control loop

margin for $G \to \infty$. When the gain decreases on and on, that means a rising frictional damping, the pole which becomes conjugate-complex walks along the semicircle as indicated by the arrows in Fig. 6. Here, the control response will provide a transient overshoot. However, for an exemplary marked gain value 0.065 (about 15 times smaller than the nominal one) the time constant of the closed-loop control remains still adequate.

Closing, it can be seen that the designed robust feedback control allows large-range uncertainties of frictional damping and that about 100 times in magnitude. The preferred gain variations, with regard to the control overshoot, are indicated in Fig. 6 by the dashed line and low-bounded by 0.17.

D. Control evaluation

Three different controllers: the robust PI one discussed before in Section IV-C, the same PI control combined with the feedback-based friction observer (PI+FBFO), and finally the same PI control combined with the feed-forward friction observer (PI+FFFO) have been evaluated and compared with each other. Both, the PI+FBFO and PI+FFFO control implies one and the same identified 2SEP friction model. Recall that when applying the PI+FBFO control the measured velocity is used and the toggle is switched to "1" (see Fig. 1). The PI+FFFO control uses the reference velocity value and the toggle is switched to "0" correspondingly.

The reference velocity profile taken to evaluate the control performance is shown in Fig. 7. The designed motion trajectory composes the multi-sinus (0.01–10 Hz) enveloped by a sigmoid function so that both, high and low relative velocities between 0.2 rps and 15 rps are present. Note that the relative motion changes persistently its direction, – an operating mode at which the compensation of dynamic friction is particularly relevant. Further it can be suggested that the velocity control performance like step-response is also of great importance, especially in context of a cascade positioning control. However here, the main challenges would be first to overcome the break-away conditions as fast as possible, and second to avoid an overcompensation during the step settling time. An accurate observation and compensation of friction dynamics appears to be subordinate in the face of step-related control tasks.

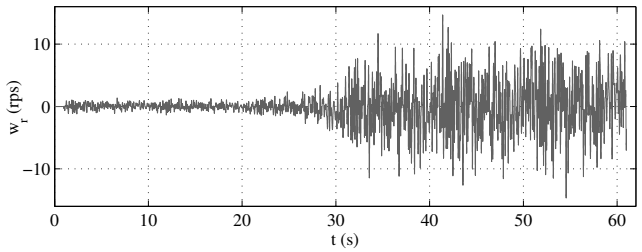

Fig. 7. Reference velocity profile taken for the control evaluation

Several cut-outs taken exemplarily from the evaluated velocity profile are depicted in Fig. 8 for the PI and PI+FFFO control. For lower relative velocities shown in both upper images it is evident that the PI control induces a substantial control lag each time the motion direction changes. At lowest reference peaks the PI control even misses the action and the velocity response remains close to zero. A clearly visible control lag is also at higher velocities as shown in both bottom images in Fig. 8. It can be recognized that the PI+FFFO control exhibits a definitely better follow-up performance for both low and hight velocities.

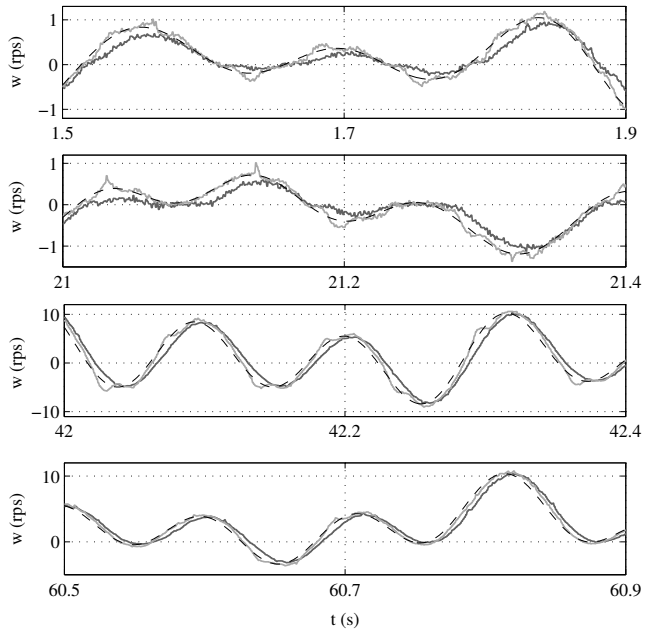

Fig. 8. Cut-outs of evaluated velocity profile: black dash line – reference, light grey solid line – PI+FFFO control, dark grey solid line – PI control

The evaluated error histograms are shown in Fig. 9. It is evident that the narrowest error spread is in case (c), PI+FFFO control. As expected, the simple PI control shown in (a) exhibits the largest error spread. Also the shape of the error histograms argues for the superior follow-up performance of the PI+FFFO control. Its error distribution is most closer to the normal one and thus reveals a rather stochastic (noise-related) character of residual errors.

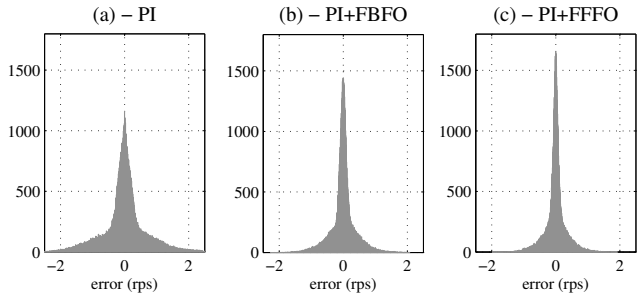

Fig. 9. Error histograms of the evaluated controls

In order to compare the follow-up control performance in a quantitative way the following error metrics

ISE – Integral Square Error ($\mathbf{e}^T\mathbf{e}$),
MAE – Mean Absolute Error ($1/n\sum_1^n|e_i|$),
MAX – Maximal Absolute Error,
STD – Error Standard Deviation

have been selected for evaluation. For a better reproducibility each evaluated metric is normalized by its minimal realization when comparing the controls between each other. Thus, the minimal realization, that means the highest rating of a particular metric, achieves the 100 % value. The evaluated control metrics are listed in Table II.

TABLE II
EVALUATED CONTROL METRICS

Control	ISE %	MAE %	MAX %	STD %
PI	442	222	159	210
PI+FBFO	146	122	114	120
PI+FFFO	100	100	100	100

It is evident that the PI+FFFO control proves to be superior and that for all evaluated control metrics. Here one realizes that also the PI+FBFO control yields a considerable improvement comparing to the simple PI one without any friction compensation. However, the computed friction value which is lagged due to the measured output velocity, as mentioned before, reveals the PI+FBFO control as inferior comparing to the PI+FFFO one. Furthermore it can be noted that a feedback friction computation offers additional disadvantages since an implemented friction model can be sensitive to the quality of the measured output velocity. Here it is worth noting that the 2SEP friction model is robust against highly disturbed velocity signals (see [8]) and can be easily applied in both ways without auxiliary filtering.

V. CONCLUSIONS

This paper has introduced a novel feed-forward friction observer (denoted by FFFO) which uses the 2SEP dynamic friction model. The main idea which distinguishes the FFFO from a feedback-based friction observer (denoted by FBFO), like one proposed in [13], is to compute the dynamic friction state using the reference and not output velocity value. At the same time, the observation of the dynamic friction is carried out using the control error which drives the friction state by means of a properly selected observation function. The stability of the FFFO-based control loop is shown by analyzing the corresponding system dynamics. For an experimental motion system with multiple coupled frictional surfaces the first-order dynamics with nonlinear friction and time delay has been identified. The robust linear feedback loop has been designed as a reference control system. This one has been evaluated in comparison to the FBFO- and FFFO-based control which use the same 2SEP friction model. The evaluated motion profile with varying amplitudes and frequencies discloses the FFFO-based control as clearly superior.

REFERENCES

[1] B. Armstrong-Helouvry, P. Dupont, and C. C. de Wit, "A survey of modeling, analysis tools and compensation methods for the control of machines with friction," *Automatica*, vol. 30, pp. 1083–1138, 1994.
[2] V. Lampaert, J. Swevers, and F. Al-Bender, "Comparison of model and non-model based friction compensation techniques in the neighbourhood of pre-sliding friction," in *Proc. 2004 American Control Conference*, 2004, pp. 1121–1162.
[3] C. C. de Wit, H. Olsson, K. J. Aström, and P. Lischinsky, "A new model for control of systems with friction," *IEEE Transactions on automatic control*, vol. 40, no. 3, pp. 419–425, 1995.
[4] K. J. Aström and C. C. de Wit, "Revisiting the LuGre friction model," *IEEE Control Systems Magazine*, vol. 28, no. 6, pp. 101–114, 2008.
[5] M. Ruderman and T. Bertram, "Friction model with elasto-plasticity for advanced control applications," in *Proc. IEEE/ASME International Conference on Advanced Intelligent Mechatronics*, 2010, pp. 914–919.
[6] F. Altpeter, M. Grunenberg, P. Myszkorowski, and R. Longchamp, "Auto-tuning of feedforward friction compensation based on the gradient method," in *Proc. American Control Conference 2000*, vol. 4, 2000, pp. 2600–2604.
[7] L. Freidovich, A. Robertsson, A. Shiriaev, and R. Johansson, "LuGre-model-based friction compensation," *IEEE Transactions on Control Systems Technology*, vol. 18, no. 1, pp. 194–200, 2010.
[8] M. Ruderman and T. Bertram, "Observer-based control strategies for compensation of dynamic friction," in *Proc. 19th IEEE Mediterranean Conference on Control and Automation*, 2011, pp. 67–72.
[9] Y. Maeda and M. Iwasaki, "Initial friction compensation by disturbance observer based on rolling friction model," in *35th Annual Conference of IEEE Industrial Electronics*, 2009, pp. 3124–3129.
[10] Z. Jamaludin, H. Van Brussel, and J. Swevers, "Friction compensation of an XY feed table using friction-model-based feedforward and an inverse-model-based disturbance observer," *IEEE Transactions on Industrial Electronics*, vol. 56, no. 10, pp. 3848–3853, 2009.
[11] A. Amthor, S. Zschaeck, and C. Ament, "High precision position control using an adaptive friction compensation approach," *IEEE Transactions on Automatic Control*, vol. 55, no. 1, pp. 274–278, 2010.
[12] M. Ruderman and T. Bertram, "FRF based identification of dynamic friction using two-state friction model with elasto-plasticity," in *Proc. IEEE International Conference on Mechatronics*, 2011, pp. 230–235.
[13] H. Olsson and K. J. Astrom, "Observer-based friction compensation," in *Proc. 35th IEEE Conference on Decision and Control*, vol. 4, 1996, pp. 4345–4350.
[14] M. Ruderman and T. Bertram, "Modified Maxwell-slip Model of presliding friction," in *Proc. 18th IFAC World Congress*, 2011, pp. 10 764–10 769.
[15] F. Al-Bender and J. Swevers, "Characterization of friction force dynamics," *IEEE Control Systems Magazine*, vol. 28, no. 6, pp. 64–81, 2008.
[16] F. Al-Bender, V. Lampaert, and J. Swevers, "Modeling of dry sliding friction dynamics: From heuristic models to physically motivated models and back," *Chaos*, vol. 14, no. 2, pp. 446–460, 2004.